Plant Science 304 (2021) 110809

Contents lists available at ScienceDirect

Plant Science

journal homepage: www.elsevier.com/locate/plantsci

Research Article

Transition of aromatic volatile and transcriptome profiles during melon fruit ripening

Yukihiro Nagashima [a], Kai He [b], Jashbir Singh [a], Rita Metrani [a], Kevin M. Crosby [a], John Jifon [a,c], G.K. Jayaprakasha [a], Bhimanagouda Patil [a,d], Xiaoning Qian [b,e,f], Hisashi Koiwa [a,g,*]

[a] Vegetable and Fruit Improvement Center, Department of Horticultural Sciences, Texas A&M University, College Station, TX, 77843, USA
[b] Department of Electrical and Computer Engineering, Texas A&M University, College Station, TX, 77843, USA
[c] Texas A&M AgriLife Research and Extension Center, 2415 E Business 83, Weslaco, TX, 78596, USA
[d] Department of Food Science and Technology, Texas A&M University, College Station, TX, 77843, USA
[e] TEES-AgriLife Center for Bioinformatics & Genomic Systems Engineering, Texas A&M University, College Station, TX, 77843, USA
[f] Department of Computer Science and Engineering, Texas A&M University, College Station, TX, 77843, USA
[g] Molecular and Environmental Plant Sciences, Texas A&M University, College Station, TX, 77843, USA

ARTICLE INFO

Keywords:
Cucumis melo
Aromatic volatiles
Carotenoids
Apocarotenoids
Lipids
RNA-seq

ABSTRACT

Melon (*Cucumis melo L.*) is an important diploid crop with a wide variety of flavors due to its distinct aromatic volatile organic compounds (VOC). To understand the development of VOC profiles during fruit development, we performed metabolomic and transcriptomic analysis of two cantaloupe varieties over the course of fruit development. A total of 130 metabolites were detected in fruit samples, and 449014207 reads were mapped to the melon genome. A total of 4469 differentially expressed genes in fruits were identified and used to visualize the transition of VOC and transcriptomic profiles during the fruit development. A shift of VOC profiles in both varieties was observed from early-fruit profiles enriched in C5-C8 lipid-derived VOCs to late-fruit profiles abundant in C9 lipid-derived VOCs, apocarotenoids, and esters. The shift coincided with the expression of specific isoforms of lipid and carotenoid metabolizing enzymes as well as transcription factors involved in fruit ripening, metabolite regulation, and hormone signaling.

1. Introduction

Muskmelon (*Cucumis melo* L.) is one of the important horticultural crops of the Cucurbitaceae family. Global production of melon fruits was approximately 27 million tons, with the United States production yielding 872080 tons and ranking sixth overall [1]. Of several varieties of melons produced in the United States, cantaloupe with orange-fresh fruits is the most popular melon. Together with honeydew, melons were grown in 33,510 ha and had an economic value of US$ 395 million [2]. Melon is diploid (2n = 24) and has an approximate genome size of 450 Mbp [3]. A high-quality reference genome of melon was first released in 2012 [4], and the latest version (DHL92 v4.0) covers 358 Mbp pseudomolecules [5].

Proper development of the fruits is essential for the quality of melon fruits. The life cycle of cantaloupe is 80–120 days, and the fruit ripening takes 35–45 days after flowering. After pollination, the melon fruits drastically increase their volume and then turn soft. Melon varieties are classified into two groups, climactic and non-climactic. Climactic melon has a peak of ripening, controlled by an increase of respiration and the plant hormone ethylene, and non-climatic melon has no such peak. Ethylene synthesis is controlled by two major enzymes, ACC synthase and ACC oxidase, and ethylene affects the expression of genes related to fruit ripening [6]. The climactic reaction causes chlorophyll degradation, abscission, synthesis of aroma volatiles, and softening of fresh. The non-climactic ripening reaction causes sugar accumulation, loss of acidity, and coloration of the flesh [7].

The aroma of melon fruit is a complex mixture of volatile organic compounds (VOC), including alcohols, aldehydes, amino acid esters, ketones, and hydrocarbons of various origin [8]. Together with soluble metabolites, fruit aroma affects the consumer preferences of melons [9]. A significant number of aromatic volatiles, including straight-chain esters, alcohols, and aldehydes, are produced as cleavage products of

* Corresponding author at: Vegetable and Fruit Improvement Center, Department of Horticultural Sciences, Texas A&M University, College Station, TX, 77843, USA.
E-mail address: koiwa@tamu.edu (H. Koiwa).

https://doi.org/10.1016/j.plantsci.2020.110809
Received 3 November 2020; Received in revised form 16 December 2020; Accepted 18 December 2020
Available online 25 December 2020

carotenoids and polyunsaturated fatty acids [10]. Beta-carotene, a precursor of vitamin A, represents the characteristic orange flesh color of the cantaloupe fruits. Carotenoid synthesis pathway is composed of multiple enzymes, e.g., phytoene synthase (PSY), phytoene desaturase (PDS), and ζ-carotene desaturase (ZDS). A primary factor in carotenoid accumulation in the melon fruit is a polymorphism in Orange (OR) gene, a regulator protein of chromoplast differentiation in fruits, where a conserved amino acid Arg^{108} is replaced with His [11]. The critical enzymes for producing the volatile apocarotenoids are Carotenoid Cleavage Dioxygenase CCD1 and CCD4, which specifically cleave the 9, 10 (9′, 10′) double bonds of C40-carotenoids. This cleavage results in volatile C13-apocarotenoid, such as α- and β-ionone and C14 dialdehyde [12].

Polyunsaturated fatty acids (PUFA) are another source of aromatic volatiles. The combined action of lipase and lipoxygenase (LOX) will initiate the oxylipin production, which will be further processed by a suite of enzymes to generate various linear and cyclic VOC [13]. LOX isoforms have regiospecificity and are classified to 9-LOX or 13-LOX, generating (9S)- and (13S)-hydroperoxides of linoleic and linolenic acids [14]. Accordingly, downstream enzymes, an atypical P450 subfamily: the CYP74, are distinguished into 9- or 13-hydroperoxide-specific or unspecific isoforms, generate cyclic allene oxides (allene oxide synthase), produce lipid cleavage products (fatty acid hydroperoxide lyase) or divinyl esters (divinyl ester synthase) [15]. HPLs are responsible for the production of green leafy volatiles (GLVs), which typically are linear C6 volatiles (3Z)-hexenal, (3Z)-hexenol, and (3Z)-hexenyl acetate, which confer grassy aroma to the melon fruits [16].

Metabolomic studies have revealed diverse chemical profiles associated with different melon varieties [17]. Also, molecular studies showed transcriptome in different melon varieties and their dynamics during the ripening process [18–20]. Still, little has been documented about the relationship of ripening dynamics of melon metabolites and gene expression. In this study, we analyzed the fruit development of popular cantaloupe varieties by RNA-seq and metabolite profiling. F39, a breeding line of commercially important western-shipper cantaloupe, and Da Vinci, a commercial Tuscan variety, were chosen for analysis. Aromatic VOC and transcript profiling in different fruit ripening stages revealed the transition of emitted VOC and dynamism of fruit specific transcripts during the melon fruit development.

2. Materials and methods

2.1. Plant materials

Two muskmelon cultivars, namely: a Western-shipper type (Cantaloupe F39) [21] and a Tuscan type (Da Vinci, TTDV; Sakata Seed America, Morgan Hill, CA, U.S.A.) were used in the current study. The study was conducted during the spring growing season (March–June) in fields located at the Texas A&M AgriLife Research Center – Texas A&M University System in Weslaco, Texas (latitude 26° 9' N, longitude 97° 57' W; elevation 21 m). This region has a humid sub-tropical climate regime with over 300 frost-free days. The predominant soil type in the study field is a Hidalgo sandy clay loam (pH 7.2–8.3). Six-week-old seedlings were transplanted on March 15, 2019 and managed following standard commercial practices for melon production which include raised beds covered with plastic mulch and subsurface drip irrigation. Irrigation scheduling was based on soil moisture depletion measured with granular matrix soil moisture sensors (Watermark®, Irrometer Co., Riverside, CA). Pre-plant soil analyses indicated adequate calcium (Ca) magnesium (Mg) and potassium (K) levels (3.7, 0.38 and 0.36 g kg^{-1} respectively). Through the growing season the crop received (125 kg N·ha^{-1} using urea ammonium nitrate) in split doses. A micronutrient fertilizer (Foli-Gro™ Micro-Mix; Wilbur–Ellis, Co, Fresno, CA, USA) containing magnesium (Mg, 0.5 g kg^{-1}), boron (B, 2.5 g kg^{-1}), copper (Cu, 2.5 g kg^{-1}), iron (Fe, 5.0 g kg^{-1}), manganese (Mn, 5.0 g kg^{-1}), molybdenum (Mo, 0.025 g kg^{-1}), and zinc (Zn, 20 g kg^{-1}) was applied with foliar pesticide treatments at the vine elongation stage at a rate of 4.6 L·ha^{-1}. Representative weather conditions during the 2019 growing season were: air temperature, 25.7 °C; air relative humidity, 57.9 %; solar radiation, 18.4 MJ m^{-2}·d^{-1}; and total precipitation, 361.7 mm.

Leaf and fruit samples were obtained at various growth stages for analyses. Total RNA samples were prepared from 14-day-old leaves (S19, S20, S21) and fruit flesh harvested at 20–25 days (S1, S2, S3, S10, S11, S12), 30–35 days (S4, S5, S6, S13, S14, S15), 40 days (S7, S8, S9, S16, S17, S18), and 45 days (S59, S60, S61, S62, S63, S64) after flowering. The plant tissues were flash-frozen in liquid nitrogen, ground with a mortar and a pestle, and stored at -80 °C until use.

2.2. RNA library sequence

Approximately 0.25 g of the powdered, frozen tissues were mixed with 1 mL of Trizol reagent (ThermoFisher) and incubate for 5 min. The solution was mixed with 0.5 mL of chloroform and centrifuged at 12,000 *g* for 10 min after incubation for 5 min. The aqueous phase was mixed with 350 μL of ethanol and loaded to an EconoSpin column (Epoch Life Science), and centrifuged at 8000 *g* for 40 s. The column was washed twice with 450 μL of 3 M sodium acetate and with 320 μL of 70 % ethanol. RNA was eluted with 30 μL of RNase-free water. Subsequently, RNA samples were treated with DNase and cleaned up with phenol-chloroform extraction and ethanol precipitation. cDNA libraries were synthesized using Universal Plus mRNA-seq with NuQuant Kit (NuGen) according to the manufacturer's protocol and analyzed by Illumina NovaSeq 6000 with 150 bp paired-end mode.

2.3. RNA read alignment and clustering analysis

Reads were aligned to the Melonomics genome sequence: CM3.6.1_pseudomol.fa (https://www.melonomics.net/melonomics.html#/download) along with the annotation reference: CM4.0.gtf, using STAR (v2.5.4b) [22] with two allowed mismatches per pair at maximum for the alignment (outFilterMismatchNmax = 2), which successfully generated 7.9–23 million aligned reads/fruit corresponding to 67–91 % of the total sequence reads/fruit. The uniquely mapped reads were used to count the number of reads per gene while mapping, considering overlapping one and only one gene according to its genome location. Both ends of the paired-end reads were checked for overlaps.

Principal Component Analysis (PCA) [23], based on the gene expression data using the scikit-learn package (v0.22.2.post1) [24], revealed the relations between samples from different stages (Fig. 1A). Both F39 and TTDV samples exhibited clear separations for early- and late-stage samples with 1 sample in the middle. Therefore, subsequent analyses were performed using samples grouped into two categories (early and late). Early and late groups for F39 were [S1, S2, S3, S4] and [S5, S7, S8, S9, S59, S60, S61], respectively, and for TTDV were [S10, S11, S12, S13, S14, S15] and [S16, S18, S62, S63, S64], respectively.

2.4. Analysis of differentially expressed genes

Differential expression (DE) analysis was performed to identify genes that are significantly differentially expressed in the fruits at different development stages relative to leaves using edgeR (v3.12.1) [25], based on the gene quantification measured by STAR (v2.5.4b) [22]. Differentially expressed gene (DEG) was identified if its expression significantly changed (adjusted p-value < 0.01 and the absolute value of log_2 fold-change > 3). DEGs were termed as "common fruit gene" if a DEG was differentially expressed in all fruit stages; otherwise it was called "stage-specific gene." We calculated the correlation among samples using the pairwise Pearson correlation coefficients using the R function "cor" [26] based on the log_2 expression level of "stage-specific genes" and "common fruit genes," respectively, and visualize the correlation by the heatmaps using the R package "gplots" [27].

To understand the dynamism of DEG expression patterns in fruit

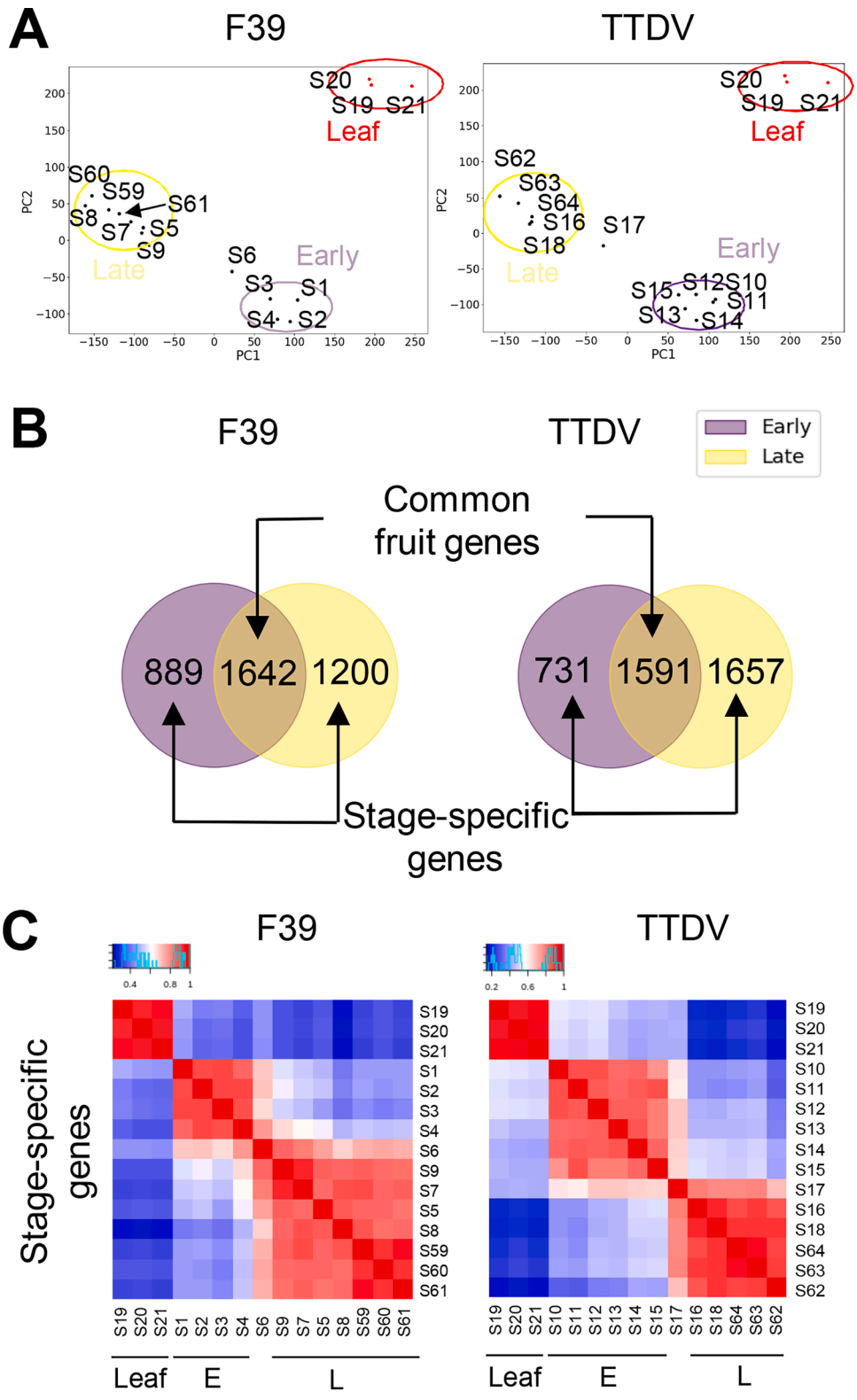

Fig. 1. Global assessment of transcriptomic data from melon fruit samples. A) PCA analysis indicated three distinct groups in transcriptome datasets, corresponding leaf, the early stage, and the late stage. B) Venn diagram of genes differentially expressed between leaf and fruit samples. DEGs identified in both fruit stages are denoted as "Common fruit genes." Other DEGs are denoted as "Stage-specific genes." C) Hierarchical clustering of RNA-seq data from each fruit sample. Expression levels of stage-specific DEG were used to calculate distances. E and L denote early (E) and late (L) maturity stages.

stages, we performed k-means clustering analysis and visualized the trajectories of gene expression levels. Specifically, for each DEG, the log2 fold-change, computed in edgeR based on the expression levels at early and late stages compared to the leaf samples, were first used to group the "common fruit genes" and "stage-specific genes" separately based on their up- or down-regulated patterns at the early and late stage. For each pattern, we further performed k-means clustering [28] using the built-in R function (v3.6.0) [26], run with 100 times of different centroid seeds for random k-means clustering initializations. The number of clusters (k) for each pattern group was determined by the ELBOW method [29], where the k-means clustering algorithm was run for different values of k, and the total within-cluster sum of squares (wss) of Euclidean distances was computed for each k. The curves of wss over different k values were plotted, where the location of a bend (knee) is

generally considered an indicator of the appropriate number of clusters [29].

The gene ontology (GO) enrichment analysis was performed using a plant regulatory data and analysis platform "PlantRegMap" (http://plantregmap.cbi.pku.edu.cn/). The pathways were determined as "significant" if their p-values < 0.01.

2.5. qPCR analysis

Samples used were leaf (S19, S20, S21), F39 early (S1, S2, S3), F39 late (S59, S60, S61), TTDV early (S10, S11, S12), and TTDV late (S62, S63, S64). For reverse transcription, 500 ng of the total RNA was used for cDNA synthesis. qPCR was conducted using BrightGreen 2x qPCR MasterMix-No Dye (Applied Biological Materials Inc.), 1/20 of the reverse transcription products per duplicate reactions, and the primers listed in the Supplemental Data 1 according to the manufacturer's protocol. The relative expression was calculated by the ΔCt method using 18 s rRNA as the reference gene.

2.6. Sample preparation and chromatographic method for the quantitation of amino acids

Amino acids were analyzed according to the published protocol [30]. Briefly, melon fruit pulp was cut into small pieces and blended for 1 min. Fifteen grams of blended samples were mixed with 10 mL of methanol. The sample contents were homogenized (2 min) at 10,000 rpm (850 Homogenizer, Thermo Fisher Scientific, Waltham, MA) followed by sonication (30 min). The extract was centrifuged (7826 x *g*) for 10 min, and supernatants were collected using Whatman filter paper No. 1. The same extraction procedure (2 × 7 mL) was repeated to ensure the maximum recovery of analytes. Supernatants were pooled, and the final volumes were recorded.

An aliquot (350 μL) of the extracted sample was mixed with 300 μL of sodium borate buffer (5 mM), 50 μL of diamino heptane (internal standard 500 ppm), and 125 μL DNS-CL (0.01 % in acetone). The reaction mixture was vortexed, and the mixture was incubated for 30 min in a water bath (60 ± 1 °C). An aliquot of 2 N acetic acid (50 μL) was added to stop the derivatization reaction. The reaction mixture was then centrifuged (10,621 x *g*) for 5 min, and the supernatant was injected into the HPLC-FLD system. HPLC-FLD system comprised of a PerkinElmer Series 200 binary pump, an autosampler (Shelton, CT, U.S.A.), and an a1260 Infinity fluorescence detector (Agilent Technologies, Santa Clara, CA, U.S.A.). The detector excitation and emission wavelengths were set at 293 nm and 492 nm, respectively, for peak detection. Column Eclipse XDB-C_8 (4.6 × 150 mm, 5 μm) and mobile phase, 1% formic acid (solvent A) and acetonitrile: formic acid: TEA (solvent B; 98:1:1, v/v) with a flow rate of 0.6 mL min^{-1} at 30 °C were used.

2.7. Sample preparation and HPLC-PDA analysis of carotenoids

Melon fruit pulp was cut into small pieces and blended for 1 min (Oster Blender with 12 speeds, 450 W). The blended sample (10 g) was mixed with 10 mL of extraction solvent, $CHCl_3$: acetone (1:1). The mixture was homogenized for 2 min at 10,000 rpm and sonicated for 15 min at 5−10 °C. The extract was centrifuged at 7826 *g* for 10 min and passed through Whatman filter paper No. 1 to collect the supernatant. The residue was re-extracted twice with the above solvents (2 × 7 mL) to ensure complete extraction. The resultant supernatants were pooled and analyzed using HPLC. Carotenoids were analyzed with a Waters 1525 HPLC system (Milford, MA) equipped with a 2996 PDA detector and 717 Plus autosampler, as described [30]. Briefly, the separation was performed using a mobile phase of (A) methanol and (B) *tert*-butyl methyl ether (TBME) on a C_{30} column (3 μm, 150 mm × 4.6 mm, YMC Column, Waters Corp) with a flow rate of 0.6 mL/min. An HPLC gradient program as follows: 25–75 % B (0–12 min), isocratic for 8 min (75 % B), 75–25 % B (1 min) followed by 4 min isocratic at 25 % B. Carotenoids were monitored at 286, 350, 400, and 450 nm and Empower-2 software was used for data processing.

2.8. HS-SPME-GC-MS analysis of volatile compounds

Volatile compounds were identified using a Thermo Finnigan GC–MS (Thermo Fisher Scientific, Inc., San Jose, CA, USA) coupled with a Dual-Stage Quadrupole (DSQ II) mass spectrometer (Thermo Scientific, Austin, TX, USA). Approximately 1 g of melon pulp was weighed in GC–MS vial (20 mL) containing 30 % NaCl (1 mL) and internal standard (5 μL; nootkatone). A solid-phase microextraction (SPME) fiber coated with 50/30 μm Divinylbenzene/Carboxen/ Polydimethylsiloxane (DVB/CAR/PDMS) of 2 cm was used for extraction. Separation of compounds was achieved on a Restek Rtx-Wax column (30 m x 0.25mmID with 0.25 μm film thickness; Restek Corp., Bellefonte, PA, USA). The GC–MS sequence was set up, and the method started with the vials being placed into a thermostatic stirrer for 30 min maintained at 80 °C. Helium was used as the carrier gas at a constant flow rate of 1 mL min-1 in splitless mode. The initial oven temperature was maintained at 40 °C for 2 min and then increased to 210 °C at a rate of 5 °C/min with a holding time of 1 min and analysis time was 37 min. The inlet temperature was maintained at 225 °C. The ion source temperature and mass transfer line temperature were maintained at 285 and 280 °C, respectively. The ionization voltage was 70 eV, the mass range was 30–300 amu, and the scan rate was 11.7 scans per second. The data were recorded using Xcalibur software (v. 2.0.7., Thermo-Fisher Scientific, San Jose, CA, USA).

3. Results

3.1. Transcriptome-based maturity indexing of fruit samples

For RNA and VOC analyses, fruits of F39 and Tuscan-type da Vinci (TTDV) were harvested during the year 2018 from the field in Weslaco, TX, at different maturation stages. The set of harvested fruits consist of 12 fruit samples of three early (~20 DAP), three middle (~30 DAP), three late (~40 DAP), and three mature (~45 DAP/full slip) stages for each variety, respectively. Three leaf samples of F39 were included in the analysis as the reference. Total RNA samples extracted from the flesh of fruits and leaves were subjected to RNA-seq analysis using the Illumina Nova seq platform. The sequencing run produced a total of 79 Gb of paired-end data for 27 samples. Alignment of sequence reads to the Melon reference genome (CM.3.6.1_pseudomol.fa) using STAR (v2.5.4b) [22] successfully generated 7.9–23 million aligned reads/fruit corresponding to 74–91 % of the total sequence reads/fruit (Supplemental Data 1). Principal Component Analysis (PCA) [23] of RNA-seq data using the scikit-learn package (v0.22.2.post1) [24] revealed relations between samples from different stages (Fig. 1A). Both F39 and TTDV samples exhibited clear separations for early- and late-stage samples with 1 sample in the middle. To properly align the fruit samples in the order of maturity, we use transcriptome patterns. Fruit gene sets used for the sample indexing were differentially expressed genes (DEGs) in melon fruits using leaf transcriptome as the reference. For this purpose, samples of each variety were grouped into two subsets (early and late) according to the grouping in PCA of the whole transcriptome. Early and late groups for F39 were [S1, S2, S3, S4] and [S5, S7, S8, S9, S59, S60, S61], respectively, and for TTDV were [S10, S11, S12, S13, S14, S15] and [S16, S18, S62, S63, S64], respectively.

Fruit-specific genes were identified by differential expression analyses comparing fruit datasets with leaf datasets using edgeR (v3.12.1) [25]. DEGs were defined as the genes whose expression significantly changed (adjusted p-value < 0.01 and the absolute value of $\log_2$ fold-change > 3) in fruits relative to leaves. This analysis identified 2531 and 2842 DEGs (differentially expressed genes) for early and late F39 fruits, respectively, and 2322 and 3248 DEGs for TTDV fruits (Supplemental Data1). The total number of DEG was 3731 for F39 and 3979 for

TTDV. Of these, 1642 (F39) and 1591 (TTDV) DEGs were detected in both early and late samples and denoted as "common fruit genes." The remaining 2089 (F39) and 2388 (TTDV) DEGs were denoted as "stage-specific genes" (Fig. 1B). Overall, 4469 unique DEGs from 2 varieties were identified. To confirm the data grouping and overall DEG expression profile, RNA-seq datasets were subjected to hierarchical clustering analysis using DEGs. We calculated the correlation among the samples based on the expression levels of the stage-specific genes, and hierarchical clustering results were visualized as the heatmaps (Fig. 1C). The heatmaps showed that expression patterns of stage-specific genes are distinct in RNA-seq data for leaves, early and late stages. The samples S6 and S17 produced intermediate profiles, consistent with PCA plot results. According to the clustering, we grouped the samples as early-stage (E) and late-stage (L). Datasets S6 and S17 with intermediate profiles were excluded from the grouping.

3.2. VOC profiles in transcriptome-indexed fruit samples

To visualize the levels of aromatic VOC production during fruit development, we performed metabolite analysis, and the metabolite profiles of individual fruit samples were generated (Supplemental Data 2). To compare the overall relationship of fruit metabolite levels (μg/kg fresh weight) in two varieties, PCA was performed (Fig. 2). The first two components were able to explain 43.9 % of the variation (Fig. 2A). The PCA was interpreted according to loading scores of variables on each component (Fig. 2B). The PCA was able to cluster variables that were positively correlated, and that contributed similar information to describe the melon variety (Fig. 2A). The first two components grouped the early-stage fruits towards the left of the plot, whereas late-stage fruits were grouped towards the right of the plot. For instance, early-stage fruits had higher values of GLV/lipid derivatives, including aldehyde "green compounds," which are correlated to unripe fruits [31,32], and low values for carotenoids and brix. Late-stage fruits had higher values for carotenoids, esters, terpenoids, apocarotenoids, and alcohols,

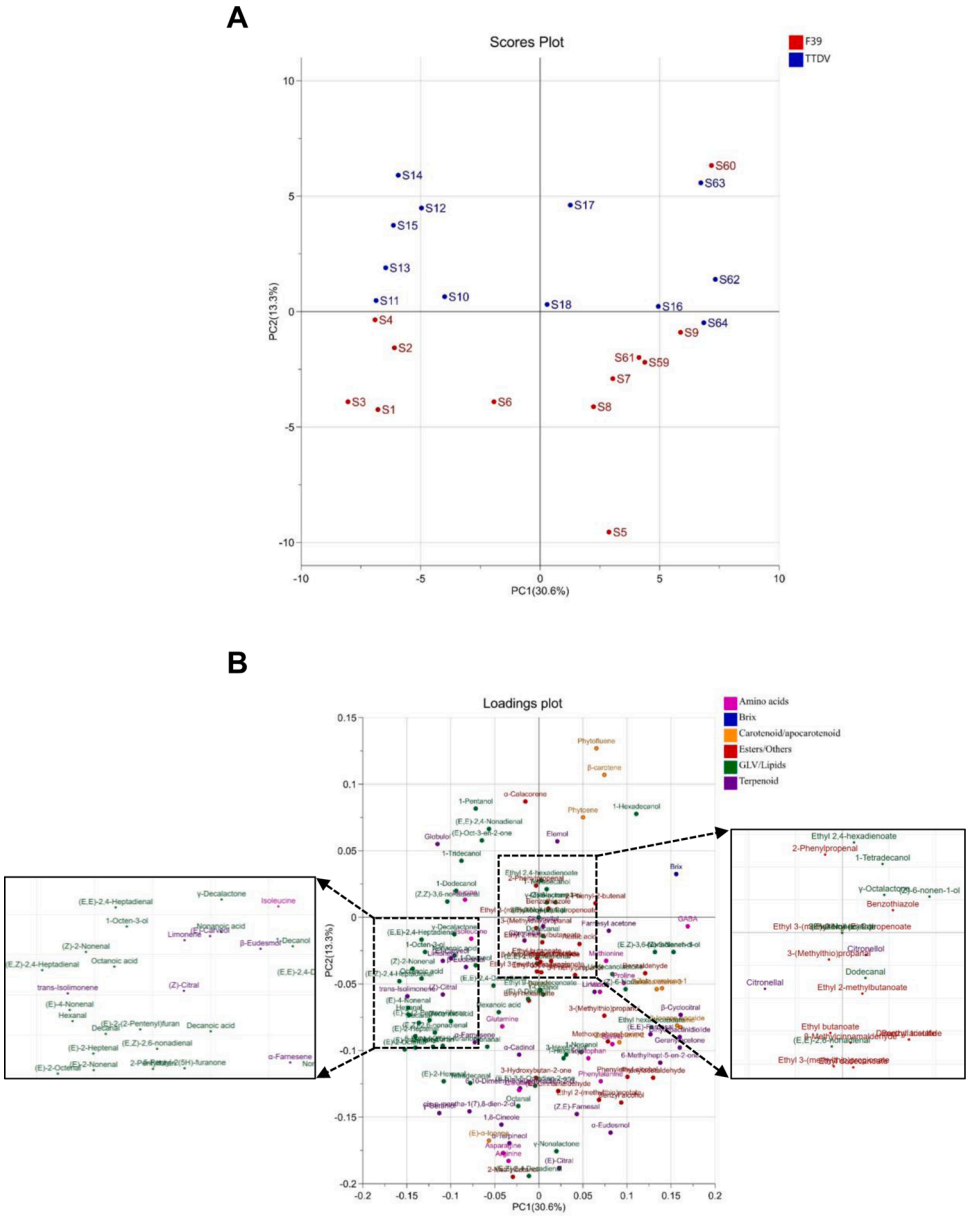

Fig. 2. Principal component analysis A) score plot B) loading plot of melon fruit metabolites at different maturity stages. Explained variance for PC 1 and PC 2 are indicated as the percentages in the X- and Y-axis, respectively.

indicating that these volatiles are highly correlated to fruity/sweet flavors.

Relative levels of individual metabolites during the fruit development were visualized using heatmap (Fig. 3). The samples were aligned using the transcriptome-based ordering of fruit maturation. The overall profiles were similar between F39 and TTDV when samples from the equivalent stages (early and mature) were compared, whereas S6 (F39) and S17 (TTDV) showed intermediate profiles. Within GLV/lipid

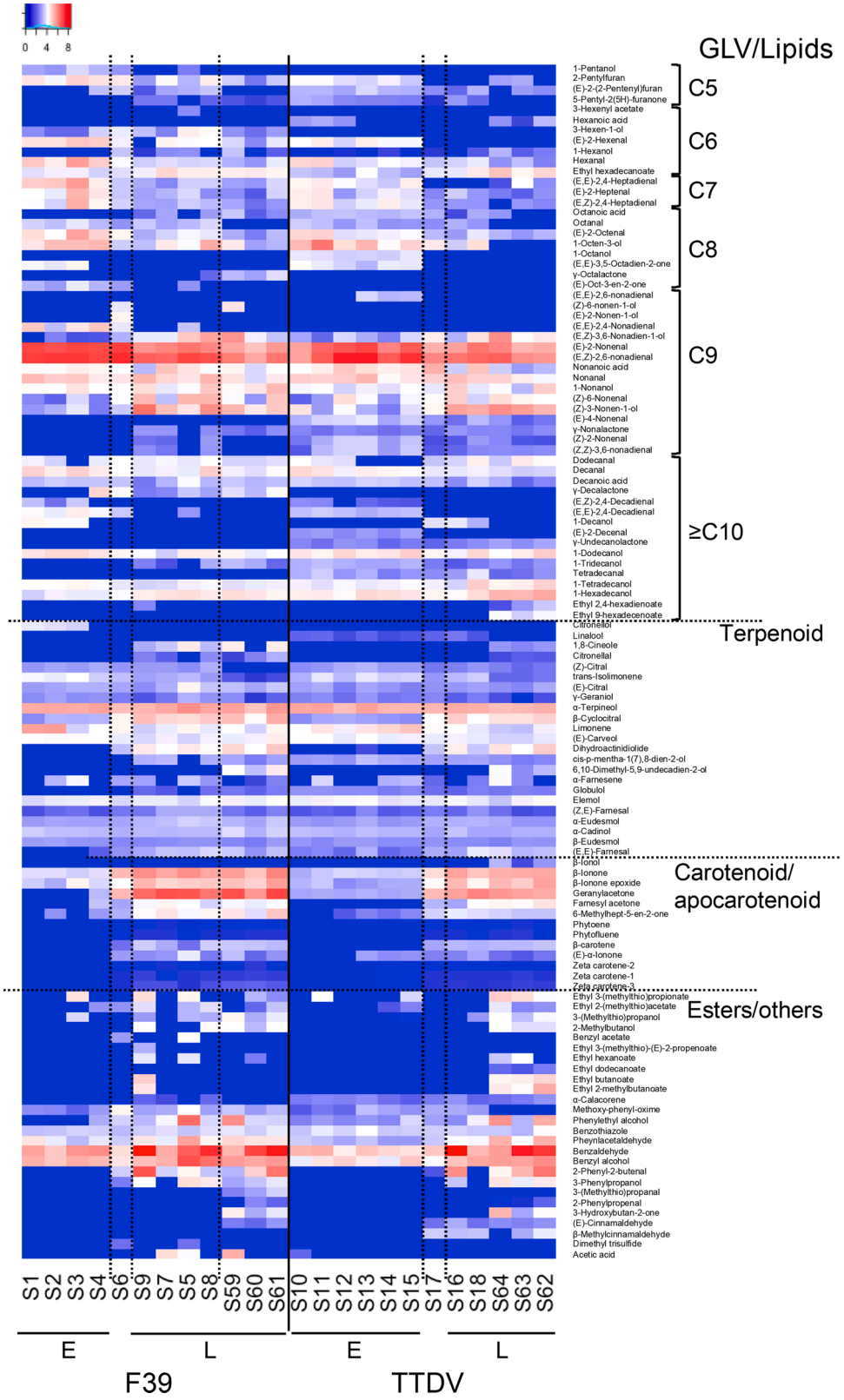

Fig. 3. Levels of aromatic VOCs in F39 and TTDV fruits in early (E) and late (L) maturity stages. The log_{10} values of metabolite levels (μg/kg) were used to generate the heatmap.

derivatives, C5-C8 VOCs are more enriched in the early stage samples whereas C9 volatiles, such as (E)-2-nonenal, (E,Z)-2,6-nonadienal, and nonanal persisted throughout the fruit development. Some C9 VOC, such as (Z)-6-nonenal and (E,Z)-3,6-nonadien-1-ol and (Z)-3-nonen-1-ol levels increased in the late-stage samples. Mono and sesquiterpenes are generally persistent throughout the fruit development, but several matured-fruit-specific/enriched terpenoids were identified, including β-cyclocitral and dihydroactinidiolide. β-carotene and apocarotenoids (β-ionone and β-ionone epoxide, 6-methylhept-5-en-2-one, farnesyl acetone, and geranylacetone), and esters (ethyl butanoate, ethyl 2-methylbutanoate, ethyl 3-(methylthio)propionate) were also abundant in mature samples. Other notable metabolites were ubiquitous benzaldehyde and benzylalcohol, and late-stage-specific 2-Phenyl-2-butenal and 3-Hydroxybutan-2-one (acetoin).

3.3. Expression levels of VOC biosynthetic pathway genes

To analyze relationships of the timing of VOC production and the expression of VOC biosynthesis pathway genes, levels of VOC biosynthetic gene expression in RNA-seq data were inspected. Genes potentially involved in VOC productions, namely, lipoxygenase (LOX), HPL, E-Z isomerase, ADH, and AAT responsible for green leafy volatiles (GLV), prenyltransferases and terpene cyclases for mono and sesquiterpenes, carotenoid biosynthetic and cleavage enzymes for apocarotenoids, and pyruvate decarboxylase and acyltransferases for ester biosynthetic genes were chosen for the analysis. Out of 125 genes identified in the melon genome v4.0, RNA-seq reads were detected for 77 genes, for which count per million (cpm) levels were shown as the heatmap (Fig. 4), and the correlations between expression of individual genes with VOC levels were shown in Table 1.

For GLV biosynthetic lipoxygenases, the expressions of LOX8 (13-lipoxygenase), LOX7 (9-lipoxygenase), and ADH10 (alcohol dehydrogenase) were observed throughout the fruit development, with a slight increase of LOX7 in the late stage samples. LOX8 and LOX18 showed a high correlation ($p < 0.01$) with GLV/lipid-derived VOCs (Table 1). The 9/13-HPL catalyzing the step following LOX showed stage specificity, MELO3C010910 expressed higher in the early stage and correlated with C9 GLVs, whereas MELO3C018413 and 3Z-2E-enal isomerase MELO3C019470 were expressed in the late stage samples and correlate with 3-Hexenyl acetate and 3-Hexen-1-ol. In the terpenoid biosynthesis

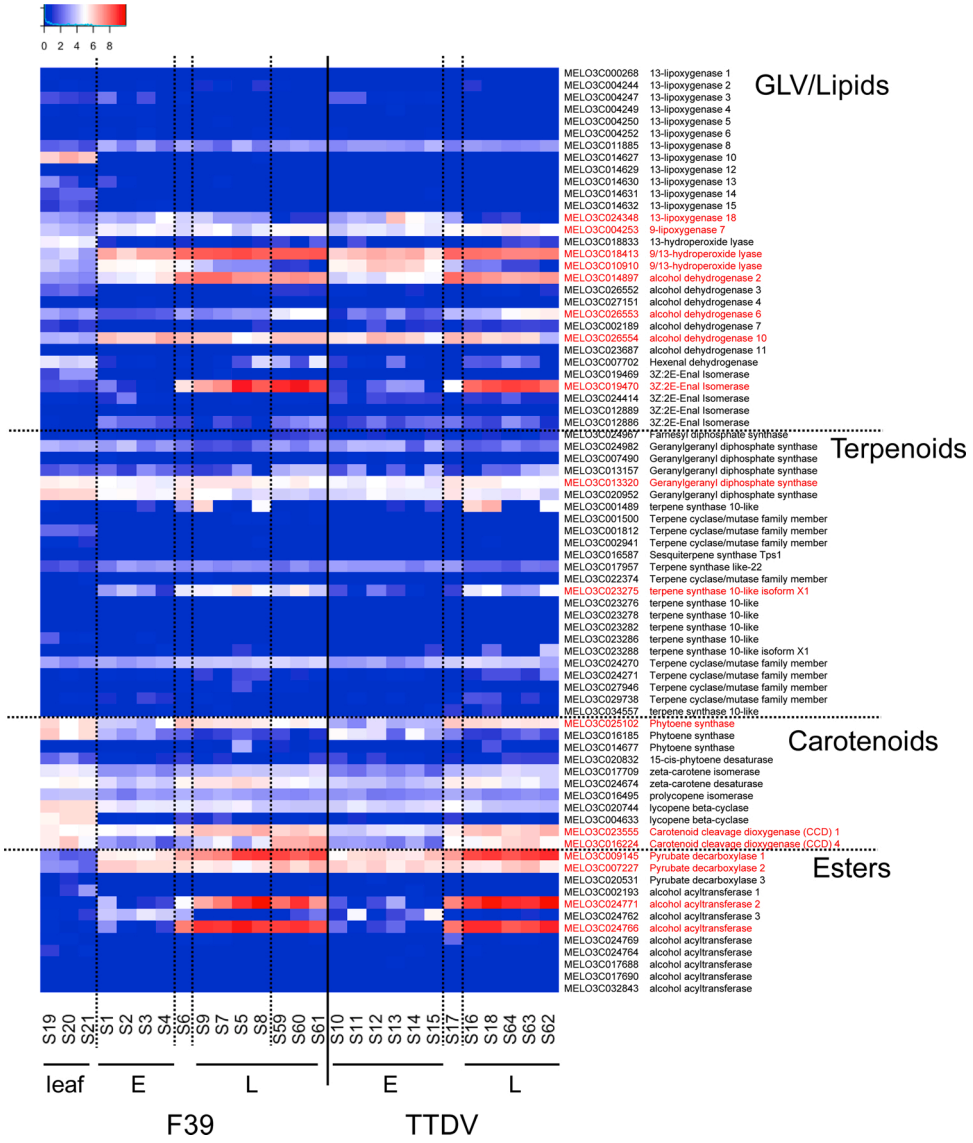

Fig. 4. Heatmap of expression profiles of genes involved in VOC biosynthesis. The log_{10} of count per million (cpm) value for each gene was used to calculate relative expression levels. E and L denote early (E) and late (L) maturity stages. Genes shown with red texts were included in RT-qPCR analysis in Fig. 6. (For interpretation of the references to colour in this figure legend, the reader is referred to the web version of this article).

Table 1
Correlation between levels of representative metabolites and potential biosynthetic transcripts.

Gene	Annotation	Compound	cor[a]	*P*-value
MELO3C011885	LOX8	3-Hexenyl acetate	0.618	1.30E-03
MELO3C024348	LOX18	(E,E)-2,6-nonadienal	0.838	3.14E-07
MELO3C024348	LOX18	(E)-2-(2-Pentenyl)furan	0.578	3.11E-03
MELO3C024348	LOX18	(E,Z)-2,6-nonadienal	0.530	7.72E-03
MELO3C024348	LOX18	(E)-4-Nonenal	0.528	8.03E-03
MELO3C018413	HPL	3-Hexenyl acetate	0.677	2.77E-04
MELO3C018413	HPL	3-Hexen-1-ol	0.645	6.63E-04
MELO3C018413	HPL	(Z)-6-Nonenal	0.592	2.29E-03
MELO3C010910	HPL	(E,Z)-2,6-nonadienal	0.639	7.79E-04
MELO3C010910	HPL	(E)-4-Nonenal	0.621	1.21E-03
MELO3C010910	HPL	(Z)-2-Nonenal	0.619	1.26E-03
MELO3C010910	HPL	(Z,Z)-3,6-nonadienal	0.564	4.07E-03
MELO3C010910	HPL	(E,E)-2,6-nonadienal	0.553	5.02E-03
MELO3C010910	HPL	(E)-2-Nonenal	0.529	7.83E-03
MELO3C026553	ADH6	1-Hexadecanol	0.751	2.37E-05
MELO3C026553	ADH6	(E)-Cinnamaldehyde	0.738	3.79E-05
MELO3C026553	ADH6	6,10-Dimethyl-5,9-undecadien-2-ol	0.688	2.02E-04
MELO3C026553	ADH6	3-(Methylthio)propanol	0.682	2.40E-04
MELO3C026553	ADH6	2-Phenylpropenal	0.642	7.12E-04
MELO3C026553	ADH6	β-Ionol	0.641	7.39E-04
MELO3C026553	ADH6	2-Methylbutanol	0.567	3.86E-03
MELO3C026554	ADH10	(E,E)-2,4-Nonadienal	0.519	9.43E-03
MELO3C019470	3Z-2E Isomerase	3-Hexenyl acetate	0.738	3.85E-05
MELO3C019470	3Z-2E Isomerase	3-Hexen-1-ol	0.477	1.84E-02
MELO3C023275	TPS10 × 1	(E)-Citral	0.842	2.54E-07
MELO3C023275	TPS10 × 1	α-Eudesmol	0.651	5.76E-04
MELO3C023275	TPS10 × 1	(Z,E)-Farnesal	0.606	1.70E-03
MELO3C023275	TPS10 × 1	1,8-Cineole	0.521	9.12E-03
MELO3C014677	PYS	(E)-α-Ionone	0.832	4.74E-07
MELO3C017709	zCI	β-Ionone	0.682	2.42E-04
MELO3C017709	zCI	β-Ionone epoxide	0.645	6.62E-04
MELO3C017709	zCI	Zeta carotene-1	0.631	9.49E-04
MELO3C017709	zCI	Phytofluene	0.598	2.05E-03
MELO3C017709	zCI	(E)-α-Ionone	0.529	7.81E-03
MELO3C024674	zCD	(E)-α-Ionone	0.693	1.75E-04
MELO3C023555	CCD1	β-Ionone	0.682	2.39E-04
MELO3C023555	CCD1	Zeta carotene-1	0.659	4.59E-04
MELO3C023555	CCD1	(E)-α-Ionone	0.624	1.13E-03
MELO3C023555	CCD1	Zeta carotene-2	0.574	3.38E-03
MELO3C023555	CCD1	β-carotene	0.568	3.81E-03
MELO3C023555	CCD1	Phytofluene	0.552	5.14E-03
MELO3C023555	CCD1	β-Ionone epoxide	0.524	8.55E-03
MELO3C016224	CCD4	Zeta carotene-3	0.680	2.56E-04
MELO3C016224	CCD4	β-Ionone epoxide	0.642	7.26E-04
MELO3C016224	CCD4	Phytofluene	0.600	1.96E-03
MELO3C016224	CCD4	β-Ionone	0.571	3.55E-03
MELO3C016224	CCD4	Zeta carotene-1	0.550	5.41E-03
MELO3C016224	CCD4	Phytoene	0.527	8.14E-03
MELO3C016224	CCD4	β-carotene	0.521	9.03E-03
MELO3C024771	AAT2	Ethyl hexadecanoate	0.604	1.79E-03
MELO3C024766	AAT	3-Hexenyl acetate	0.731	4.88E-05
MELO3C024766	AAT	Benzyl acetate	0.721	7.04E-05

[a] Correlation coefficient.

pathway, isoforms of geranylgeranyl diphosphate synthases (MELO3C013320 and MELO3C020952) and terpene cyclase (MEL3C024270) were more prevalent throughout the fruit development, and terpene synthase 10-like isoform X1 (MEL3C023275) showed late stage-specific expression correlating with several mono and sesquiterpenoids. For carotenoid/apocarotenoid biosynthesis, isoform-specific expression was observed with phytoene synthase, and enhanced expression of ζ-carotene isomerase and ζ-carotene desaturase in the late stage. Furthermore, significant correlations were observed with carotenoid cleavage dioxygenases (CCD) (MELO3C023555 and MELO3C016224) and carotenoid/apocarotenoid levels. Finally, high expression of alcohol acyltransferases isoforms (MELO3C024771 and MELO3C024766) in the late stage correlated with ethyl hexadecanoate and benzyl acetate ester productions in mature fruits.

3.4. Analysis of global transcriptome shift during the transition

The whole transcriptome and metabolite PCA indicated that the early- and late-stage fruits are under distinct physiological states and have distinct gene expression profiles. To understand the transcriptome-wide dynamism in the transition of fruit stages, we performed k-means clustering analysis of DEG expression patterns [28] and visualized trajectories of gene expression levels using the built-in R function (v3.6.0) [26] with the ELBOW method [29] (Fig. 5A). We grouped DEGs into 10 and 6 groups for stage-specific and common fruit genes, respectively (Supplemental Data 3-1). These clusters were termed as ssC1-ssC10 and cfC1-cfC6 for each of F39 and TTDV. Corresponding clusters in each variety showed similar expression profiles; for example, DEGs in ssC1 in F39 and TTDV exhibited overall upregulation and upward trends during fruit maturation relative to the leaf samples. When we compared genes included in each cluster of F39 and TTDV, the corresponding clusters in each variety showed the highest level of overlap, suggesting overall gene expression pattern is conserved between F39 and TTDV. Fig. 5B provides the heatmap visualization based on the overlap percentage of the

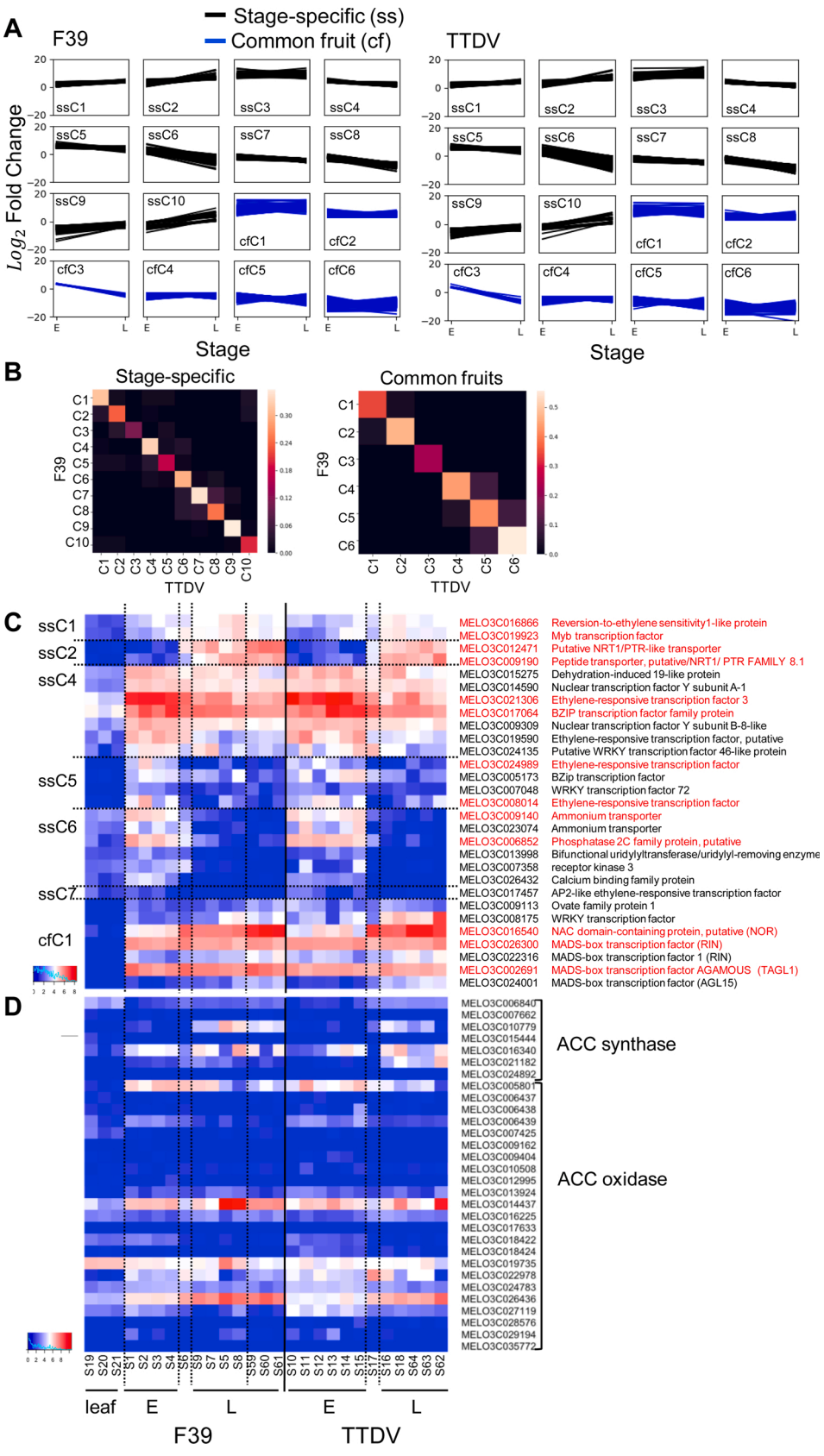

Fig. 5. Expression profiles of DEG in melon fruits. A) K-means clustering of stage-specific (ss, black lines) and common fruits (cf, blue lines) DEGs. B) Heatmap analysis of common transcripts shared between F39 and TTDV in each cluster identified in (A). C) Expression profile of regulatory proteins commonly identified in individual gene clusters. D) Expression profile of ethylene biosynthetic genes prepared as (C). The log_{10} of count per million (cpm) value for each gene was used to calculate relative expression levels. Genes shown with red texts were included in RT-qPCR analysis in Fig. 6. (For interpretation of the references to colour in this figure legend, the reader is referred to the web version of this article).

corresponding cluster pairs of F39 and TTDV. The DEGs overlapping between corresponding clusters were summarized in Supplemental Data 3-1.

To determine if a specific gene expression signature is associated with biological functions, we conducted gene ontology enrichment analysis for each cluster (Supplemental Data 3-2). The notable enrichments were found with photosynthesis-related GOs (cfC4, cfC5, cfC6), ABA signaling (ssC1, ssC6), peptide transport (ssC2), transcription (ssC4, ssC5), ammonium transport (ssC6), protein kinase/auxin signal/molybdate transport (ssC7), aminoacyl tRNA synthesis (ssC9), ovary development (cfC1). Heatmap of expression levels for selected regulatory proteins such as transcription factors (TFs) are shown in Fig. 5C. Higher expression of genes below was found at the early stage: MELO3C021306 (Ethylene-responsive transcription factor 3, ERF3), MELO3C017064 (BZIP transcription factor family protein), MELO3C009309 (Nuclear transcription factor Y subunit B-8, NFYB8-like), MELO3C019590 (ERF), MELO3C006852 (Phosphatase 2C family protein). On the other hand, MELO3C008175 (WRKY transcription factor) showed higher expression at the late stage. In the cfC1 cluster, five ripening regulator genes were identified. MELO3C016540 (NAC domain-containing protein) is a homolog of tomato *NOR* (*NO RIPENING*), and its expression gradually increased during the fruit development. Four MADS-box TFs were found encoding 2 *RIN* (*RIPENING INHIBITOR*) homologs and two Agamous-like proteins (TAGL1 and AGL15). One of RIN homolog and TAGL1 showed high expression throughout the development, whereas AGL15 expression increased in the late stage.

Since the ripening process in many cantaloupes is regulated by ethylene production, we checked ethylene biosynthetic gene expression (Fig. 5D). Expression of aminocyclopropane carboxylate (ACC) synthase was generally weak, but several isoforms showed expression in later stage samples. Several isoforms of ACC oxidase expression showed high expression in the late-stage fruits, particularly MELO3C014437 and MELO3C026436.

One unexpected finding was the alternating expression pattern of ammonium transporters (MELO3C009140 and MELO3C023074, the early stage) and nitrate transporter NRT (MELO3C012471 and MELO3C009190, the late stage). The importance of the NRT family transporter during embryogenesis has been shown in Arabidopsis [33]. By contrast, the function of ammonium transporter in reproduction is not very clear. Female flower-specific expression of poplar AMT1;6 and pollen-specific expression of poplar AMT1;5 and Arabidopsis AMT1;4 have been reported [34,35], suggesting a specific role of AMT isoforms in reproductions.

3.5. Validation of gene expression using RT-qPCR

To confirm the expression pattern observed with RNA-seq datasets, we conducted RT-qPCR analysis of 31 selected genes (Fig. 6). Three samples were chosen from leaf, early-stage fruits, and late-stage fruits for analysis. Of 31 genes analyzed, 29 confirmed the profile suggested from RNA-seq analysis. MELO3C001489 failed to amplify in multiple samples, whereas MELO3C004253 (LOX7) levels were not consistent with the RNA-seq data and showed that LOX7 expression declined over the course of fruit development. However, the overall transcript levels detected by RT-qPCR in these samples were very low; therefore, they may not be suitable for comparing the expression levels between samples.

4. Discussion

Production of aromatic VOC in melon fruits greatly contributes to the fruit flavor and can significantly influence the consumer choices. The melon aroma has been profiled with climactic and non-climactic varieties, and more than 240 VOC has been detected [10]. Yet, little is known about how aromatic VOC profiles change during the fruit maturation. In this study, fruit samples were collected over the course of development, and metabolite profiles of fruits were determined. Also, RNA-seq data were generated using the same fruit samples to assess the correlation between levels of metabolites and transcripts in different fruit maturation stages. Our data indicated that melon fruit metabolites and transcripts undergo a clear transition from early stage to late stage

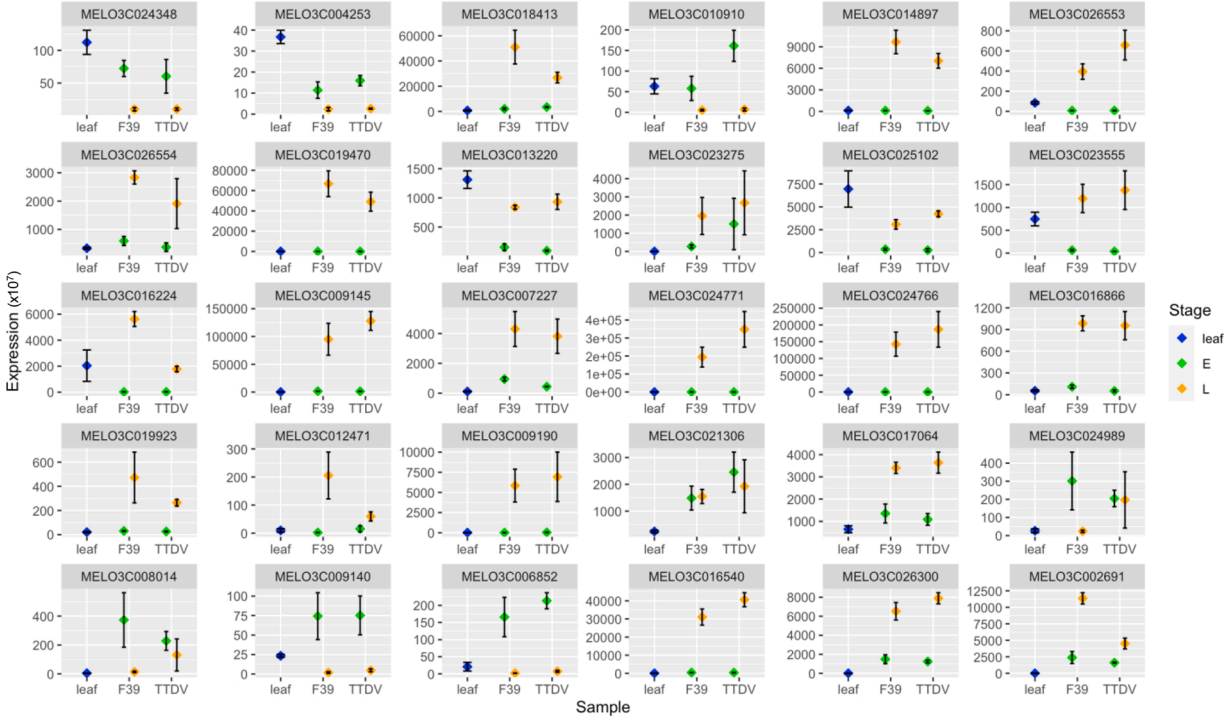

Fig. 6. Expression profiles of select DEG determined by RT-qPCR. Three RNA samples from leaves, early-stage fruits (E), or late-stage fruits (L) were used to represent each stage. Expression levels were calculated as a relative value to ribosomal 18S RNA. Bars indicate the standard error of the triplicate.

during the fruit development. The early-stage fruits were characterized by an abundance of lipid-derived GLVs, whereas late-stage fruits are rich in C9 GLVs, apocarotenoids, and esters. While gene expression does not always mean production of encoded proteins, our data are consistent with previous biochemical studies of melon fruits [36,37].

The comparison of early- and late-stage fruits revealed that stage specificities exist even within the same class of molecules, such as lipid-derived GLVs. The observed shift was caused by a decline of C5-C8 VOCs and an enrichment of C9 VOCs. Transcriptome changes associated with the shift are a decrease of 13-lipoxygenase LOX18 and 9/13-HPL (MELO3C01090) expression, an increase in 9/13-HPL (MELO3C018413) and alcohol dehydrogenease (MELO3C014897) in the late-stage fruits. Interestingly, the expression of 9-lipoxygenase (LOX7) responsible for producing 9-hydroperoxylipid, was relatively stable and observed throughout the development (or declined at the late-stage based on the RT-qPCR data). The expression of other LOX isoforms was very low in all fruit samples, suggesting LOX7, 8, and 18 could be LOX isoforms responsible for the fruit GLV biosynthesis. Also, the strong expression of 3Z:2E-enal isomerase and alcohol dehydrogenases may contribute to the derivatization of GLVs in late-stage fruits. These lipid-derived volatiles render the characteristic green and cucumber-like odors to melon fruits that may negatively affect consumer preference. By contrast, fruity flavors rendered by apocarotenoids and esters are preferred characters of mature melon fruits. Enhanced carotenoids and apocarotenoid production by the late-stage fruits in both varieties are supported by the induction of PSY isoform and carotenoid cleavage enzyme CCD1 and CCD4. CCD4 is known to cleave β-carotene at 9,10 and 9′,10′ positions to yield β-ionone and geranylacetone [38]. The CCD1 family has less strict substrate and cleavage specificities and can catabolize a wide range of all-trans- and 9-cis-carotenoids [39–42]. Ilg et al. reported that tomato CCD1A and CCD1B have a relaxed double-bond specificity and can produce geranylacetone, farnesylacetone, and citral [43]. Also, geraniol production via geranial, a cleavage product of C7–C8 double bonds of apolycopenals by rice CCD1, has been reported [44]. Therefore, our data is consistent with the model that CCD1 and CCD4 are important for the late-stage-associated apocarotenoid VOCs. Esters like ethyl butanoate and ethyl 2-methylbutanoate are likely generated from acyl CoA [45] and alcohol via the function of alcohol acyltransferase (AAT). We detected strong expression of AAT2 (MELO3C24771) and another AAT isoform (MELO3C024776). Interestingly, AAT2 in our varieties is an inactive enzyme due to T268A mutation in its amino acid sequence [46], leaving MELO3C024776 as a candidate for ester production in the melon fruit.

Clustering analysis of DEGs indicated that expression patterns of many transcripts were conserved between two varieties. Notably, fruit-specific expression of NAC and MADS-box TFs were empirically identified by this analysis, with NOR expression increasing over the fruit development. In contrast to the fruit-specific expression of developmental regulators, stage-specific transcriptional regulators include many TFs in ERF family, WRKY family, bZip family, NF-Y, MYB, and others typically related to response to environmental signals with higher expression in the early-stage in general. These TFs likely form the second level regulators in the signaling cascade to orchestrate various aspects of fruit growth and ripening, such as flavor production, wall softening, sugar metabolism. For example, a bZip TF (MELO3C005173) is homologous to tomato bZip TF ABZ1, a target of RIN [47]. Tomato ABZ1 is induced by anaerobic treatment [48]; therefore, the expression of ABZ1 in melon fruit may be related to the production of 3-hydroxybutan-2-one, which is produced by anaerobic metabolism. Tomato ABZ1 is a transcriptional repressor, and MELO3C005173 is expressed in the early stage, where 3-hydroxybutan-2-one is not produced. This implies that the production of some aromatic VOC is actively repressed at the early stage. As an important point to note, we analyzed samples from a single year in this study and therefore some variability of the results might be observed in other years. However, we identified number of similarly regulated genes in two cultivars grown in the different plots in the field, supporting the general conclusion of this study is reproducible. Overall, genes identified in our analysis likely form regulatory layers of gene expression during melon fruit ripening, influencing the fruit aromatic VOC profiles. These genes are targets of further functional characterizations and engineering using gene knockout by CRISPR/CAS9.

Funding

This research was funded by the United States Department of Agriculture-NIFA-SCRI- 2017-51181-26834 through the National Center of Excellence for Melon at the Vegetable and Fruit Improvement Center of Texas A&M University. X Qian has been supported in part by National Science Foundation awards CCF-1553281 and IIS-1812641.

Declaration of Competing Interest

The authors declare that they have no known competing financial interests or personal relationships that could have appeared to influence the work reported in this paper.

Acknowledgments

We would like to thank Ehsan Hajiramezanali (Texas A&M Electrical & Computer Engineering Department) for his assistance on metabolite correlation analysis and Drs. Charlie Johnson and Richard Metz (Texas AgriLife Research Genomics and Bioinformatics Service) for their assistance with RNA-Seq data analysis.

Appendix A. Supplementary data

Supplementary material related to this article can be found, in the online version, at doi:https://doi.org/10.1016/j.plantsci.2020.110809.

References

[1] FAOSTAT Database, United Nations, 2018.
[2] USDA-National Agricultural Statistics Service, 2014.
[3] K. Arumuganathan, E.D. Earle, Nuclear DNA content of some important plant species, Plant Mol. Biol. Rep. 9 (1991) 208–218.
[4] J. Garcia-Mas, A. Benjak, W. Sanseverino, M. Bourgeois, G. Mir, V.M. Gonzalez, E. Henaff, F. Camara, L. Cozzuto, E. Lowy, T. Alioto, S. Capella-Gutierrez, J. Blanca, J. Canizares, P. Ziarsolo, D. Gonzalez-Ibeas, L. Rodriguez-Moreno, M. Droege, L. Du, M. Alvarez-Tejado, B. Lorente-Galdos, M. Mele, L. Yang, Y. Weng, A. Navarro, T. Marques-Bonet, M.A. Aranda, F. Nuez, B. Pico, T. Gabaldon, G. Roma, R. Guigo, J.M. Casacuberta, P. Arus, P. Puigdomenech, The genome of melon (Cucumis melo L.), Proc. Natl. Acad. Sci. U. S. A. 109 (2012) 11872–11877.
[5] R. Castanera, V. Ruggieri, M. Pujol, J. Garcia-Mas, J.M. Casacuberta, An improved melon reference genome with single-molecule sequencing uncovers a recent burst of transposable elements with potential impact on genes, Front. Plant Sci. 10 (2019) 1815.
[6] H. Ezura, W.O. Owino, Melon, an alternative model plant for elucidating fruit ripening, Plant Sci. 175 (2008) 121–129.
[7] J.C. Pech, M. Bouzayen, A. Latche, Climacteric fruit ripening: ethylene-dependent and independent regulation of ripening pathways in melon fruit, Plant Sci. 175 (2008) 114–120.
[8] Y. Burger, H.S. Paris, R. Cohen, N. Katzir, Y. Tadmor, E. Lewinsohn, A.A. Schaffer, Genetic diversity of Cucumis melo, Hortic. Rev. (2009) 165–198.
[9] G. Lester, Consumer preference quality attributes of melon fruits, in: International Society for Horticultural Science (ISHS), Leuven, Belgium, 2006, pp. 175–182.
[10] M.A. El Hadi, F.J. Zhang, F.F. Wu, C.H. Zhou, J. Tao, Advances in fruit aroma volatile research, Molecules 18 (2013) 8200–8229.
[11] A. Feder, N. Chayut, A. Gur, Z. Freiman, G. Tzuri, A. Meir, U. Saar, S. Ohali, F. Baumkoler, A. Gal-On, Y. Shnaider, D. Wolf, N. Katzir, A. Schaffer, J. Burger, L. Li, Y. Tadmor, The role of carotenogenic metabolic flux in carotenoid accumulation and chromoplast differentiation: lessons from the melon fruit, Front. Plant Sci. 10 (2019).
[12] X. Hou, J. Rivers, P. Leon, R.P. McQuinn, B.J. Pogson, Synthesis and function of apocarotenoid signals in plants, Trends Plant Sci. 21 (2016) 792–803.
[13] C. Wasternack, I. Feussner, The oxylipin pathways: biochemistry and function, Annu. Rev. Plant Biol. 69 (2018) 363–386.
[14] H. Porta, M. Rocha-Sosa, Plant lipoxygenases. Physiological and molecular features, Plant Physiol. 130 (2002) 15–21.
[15] I. Feussner, C. Goebel, M. Stumpe, J.G. Carsjens, Formation of oxylipins by CYP74 enzymes for flavor production, Abstr. Pap. Am. Chem. Society 228 (2004) U56–U57.

[16] M.N. ul Hassan, Z. Zainal, I. Ismail, Green leaf volatiles: biosynthesis, biological functions and their applications in biotechnology, Plant Biotechnol. J. 13 (2015) 727–739.
[17] A. Moing, J.W. Allwood, A. Aharoni, J. Baker, M.H. Beale, S. Ben-Dor, B. Biais, F. Brigante, Y. Burger, C. Deborde, A. Erban, A. Faigenboim, A. Gur, R. Goodacre, T.H. Hansen, D. Jacob, N. Katzir, J. Kopka, E. Lewinsohn, M. Maucourt, S. Meir, S. Miller, R. Mumm, E. Oren, H.S. Paris, I. Rogachev, D. Rolin, U. Saar, J. K. Schjoerring, Y. Tadmor, G. Tzuri, R.C.H. de Vos, J.L. Ward, E. Yeselson, R. D. Hall, A.A. Schaffer, Comparative metabolomics and molecular phylogenetics of melon (Cucumis melo, Cucurbitaceae) biodiversity, Metabolites 10 (2020).
[18] H. Zhang, H. Wang, H. Yi, W. Zhai, G. Wang, Q. Fu, Transcriptome profiling of Cucumis melo fruit development and ripening, Hortic. Res. 3 (2016) 16014.
[19] A.-Y. Shin, Y.-M. Kim, N. Koo, S.M. Lee, S. Nahm, S.-Y. Kwon, Transcriptome analysis of the oriental melon (Cucumis melo L. var. makuwa) during fruit development, PeerJ 5 (2017) e2834-e2834.
[20] N. Galpaz, I. Gonda, D. Shem-Tov, O. Barad, G. Tzuri, S. Lev, Z. Fei, Y. Xu, L. Mao, C. Jiao, R. Harel-Beja, A. Doron-Faigenboim, O. Tzfadia, E. Bar, A. Meir, U. Sa'ar, A. Fait, E. Halperin, M. Kenigswald, E. Fallik, N. Lombardi, G. Kol, G. Ronen, Y. Burger, A. Gur, Y. Tadmor, V. Portnoy, A.A. Schaffer, E. Lewinsohn, J. J. Giovannoni, N. Katzir, Deciphering genetic factors that determine melon fruit-quality traits using RNA-Seq-based high-resolution QTL and eQTL mapping, Plant J. 94 (2018) 169–191.
[21] K.M. Crosby, J.L. Jifon, D.I. Leskovar, 'Chujuc', a new powdery mildew-resistant US Western-shipper melon with high sugar and β-carotene content, HortScience 43 (6) (2008) 1904–1906.
[22] A. Dobin, C.A. Davis, F. Schlesinger, J. Drenkow, C. Zaleski, S. Jha, P. Batut, M. Chaisson, T.R. Gingeras, STAR: ultrafast universal RNA-seq aligner, Bioinformatics 29 (2013) 15–21.
[23] S. Wold, K. Esbensen, P. Geladi, Principal component analysis, Chemom. Intell. Lab. Syst. 2 (1987) 37–52.
[24] F. Pedregosa, G. Varoquaux, A. Gramfort, V. Michel, B. Thirion, O. Grisel, M. Blondel, P. Prettenhofer, R. Weiss, V. Dubourg, J. Vanderplas, A. Passos, D. Cournapeau, M. Brucher, M. Perrot, É. Duchesnay, Scikit-learn: machine learning in python, J. Mach. Learn. Res. 12 (2011) 2825–2830.
[25] M.D. Robinson, D.J. McCarthy, G.K. Smyth, edgeR: a Bioconductor package for differential expression analysis of digital gene expression data, Bioinformatics (Oxford, England) 26 (2010) 139–140.
[26] R.C. Team, R: A Language and Environment for Statistical Computing, Vienna, Austria, 2013.
[27] G.R. Warnes, B. Bolker, L. Bonebakker, R. Gentleman, W. Huber, A. Liaw, T. Lumley, M. Maechler, A. Magnusson, S. Moeller, Gplots: Various R Programming Tools for Plotting Data, R Package Version, 2, 2009, p. 1.
[28] S. Lloyd, Least squares quantization in PCM, IEEE Trans. Inf. Theory 28 (1982) 129–137.
[29] R.L. Thorndike, Who belongs in the family? Psychometrika 18 (1953) 267–276.
[30] J. Singh, G.K. Jayaprakasha, B.S. Patil, Improved sample preparation and optimized solvent extraction for quantitation of carotenoids, Plant Foods Hum. Nutr. (2020) in press.
[31] J.C. Beaulieu, C.C. Grimm, Identification of volatile compounds in cantaloupe at various developmental stages using solid phase microextraction, J. Agric. Food Chem. 49 (2001) 1345–1352.
[32] B. Farneti, I. Khomenko, M. Grisenti, M. Ajelli, E. Betta, A.A. Algarra, L. Cappellin, E. Aprea, F. Gasperi, F. Biasioli, L. Giongo, Exploring blueberry aroma complexity by chromatographic and direct-injection spectrometric techniques, Front. Plant Sci. 8 (2017), 617-617.
[33] A. Almagro, S.H. Lin, Y.F. Tsay, Characterization of the Arabidopsis nitrate transporter NRT1.6 reveals a role of nitrate in early embryo development, Plant Cell 20 (2008) 3289–3299.
[34] J. Couturier, B. Montanini, F. Martin, A. Brun, D. Blaudez, M. Chalot, The expanded family of ammonium transporters in the perennial poplar plant, New Phytol. 174 (2007) 137–150.
[35] L.X. Yuan, L. Graff, D. Loque, S. Kojima, Y.N. Tsuchiya, H. Takahashi, N. von Wiren, AtAMT1;4, a pollen-specific high-affinity ammonium transporter of the plasma membrane in arabidopsis, Plant Cell Physiol. 50 (2009) 13–25.
[36] Y. Ueda, N. Fujishima, K. Chachin, Presence of alcohol acetyltransferase in melons, Postharvest Biol. Technol. 10 (1997) 121–126.
[37] C. Zhang, Y. Jin, J. Liu, Y. Tang, S. Cao, H. Qi, The phylogeny and expression profiles of the lipoxygenase (LOX) family genes in the melon (Cucumis melo L.) genome, Sci. Hortic. 170 (2014) 94–102.
[38] F.C. Huang, P. Molnar, W. Schwab, Cloning and functional characterization of carotenoid cleavage dioxygenase 4 genes, J. Exp. Bot. 60 (2009) 3011–3022.
[39] F.C. Huang, G. Horvath, P. Molnar, E. Turcsi, J. Deli, J. Schrader, G. Sandmann, H. Schmidt, W. Schwab, Substrate promiscuity of RdCCD1, a carotenoid cleavage oxygenase from Rosa damascena, Phytochemistry 70 (2009) 457–464.
[40] M. Ibdah, Y. Azulay, V. Portnoy, B. Wasserman, E. Bar, A. Meir, Y. Burger, J. Hirschberg, A.A. Schaffer, N. Katzir, Y. Tadmor, E. Lewinsohn, Functional characterization of CmCCD1, a carotenoid cleavage dioxygenase from melon, Phytochemistry 67 (2006) 1579–1589.
[41] A.J. Simkin, S.H. Schwartz, M. Auldridge, M.G. Taylor, H.J. Klee, The tomato carotenoid cleavage dioxygenase 1 genes contribute to the formation of the flavor volatiles beta-ionone, pseudoionone, and geranylacetone, Plant J. 40 (2004) 882–892.
[42] S.H. Schwartz, X. Qin, J.A. Zeevaart, Characterization of a novel carotenoid cleavage dioxygenase from plants, J. Biol. Chem. 276 (2001) 25208–25211.
[43] A. Ilg, M. Bruno, P. Beyer, S. Al-Babili, Tomato carotenoid cleavage dioxygenases 1A and 1B: relaxed double bond specificity leads to a plenitude of dialdehydes, mono-apocarotenoids and isoprenoid volatiles, FEBS Open Bio 4 (2014) 584–593.
[44] A. Ilg, P. Beyer, S. Al-Babili, Characterization of the rice carotenoid cleavage dioxygenase 1 reveals a novel route for geranial biosynthesis, FEBS J. 276 (2009) 736–747.
[45] A.G. Perez, R. Olias, P. Luaces, C. Sanz, Biosynthesis of strawberry aroma compounds through amino acid metabolism, J. Agric. Food Chem. 50 (2002) 4037–4042.
[46] I. El-Sharkawy, D. Manriquez, F.B. Flores, F. Regad, M. Bouzayen, A. Latche, J. C. Pech, Functional characterization of a melon alcohol acyl-transferase gene family involved in the biosynthesis of ester volatiles. Identification of the crucial role of a threonine residue for enzyme activity, Plant Mol. Biol. 59 (2005) 345–362.
[47] M. Fujisawa, T. Nakano, Y. Shima, Y. Ito, A large-scale identification of direct targets of the tomato MADS Box transcription factor RIPENING INHIBITOR reveals the regulation of fruit ripening, Plant Cell 25 (2013) 371–386.
[48] S. Sell, R. Hehl, Functional dissection of a small anaerobically induced bZIP transcription factor from tomato, Eur. J. Biochem. 271 (2004) 4534–4544.